

# We are IntechOpen, the world's leading publisher of Open Access books Built by scientists, for scientists

6,900

Open access books available

186,000

International authors and editors

200M

Downloads

Our authors are among the

154

Countries delivered to

TOP 1%

most cited scientists

12.2%

Contributors from top 500 universities



WEB OF SCIENCE™

Selection of our books indexed in the Book Citation Index  
in Web of Science™ Core Collection (BKCI)

Interested in publishing with us?  
Contact [book.department@intechopen.com](mailto:book.department@intechopen.com)

Numbers displayed above are based on latest data collected.  
For more information visit [www.intechopen.com](http://www.intechopen.com)



# Use of Micro-Cogeneration in Microgrids to Support Renewables

*Kemal Aygul, Burak Esenboga, Abdurrahman Yavuzdeger, Fırat Ekinçi, Tugce Demirdelen and Mehmet Tumay*

## Abstract

The use of renewable energy sources has experienced great development so as to meet energy demand. With the intention of increasing the utilization of the renewable energy sources near the demand side and compensate the fluctuation of the output power, the use of micro-cogeneration systems with solar (PV) and wind energy overcomes both technical and economic barriers. Micro-cogeneration-based hybrid PV/wind energy system can get stable power output. This new energy model also improves the power quality and significantly reduces the impact of power instability on the power network. In this study, the grid-connected hybrid PV/wind energy-based micro-cogeneration system is modeled and analyzed in detail. In order to test the performance analysis of the system, seven different scenarios are analyzed during the case studies. The analysis results show that the new energy model presents effective solutions to electrical power balance because of its properties such as safety, incombustible structure, and being eco-friendly. It is aimed at providing a broad perspective on the status of optimum design and analysis for the micro-cogeneration-based hybrid PV/wind energy system to the researchers and the application engineers dealing with these issues.

**Keywords:** eco-friendly energy, micro-cogeneration, wind turbine, photovoltaic, distributed generation, hybrid system

## 1. Introduction

Due to the increased industrialization, the electricity demand of loads is increasing. As the concerns about environmental pollution increases, the policies for environmental protection have started to become strict. To cope with increasing load demand without violating the environment protection law, the demand for distributed generation (DG) system has increased. Unlike the conventional centralized generation systems, distributed generation does not require long-distance transmission, which emits fewer pollutants. In DG systems the generator, less than 30 MW, is located near to the user side. DG provides the network operator a flexible operation. However, the integration of the DG sources into the grid is a challenging task. It requires domination of the subject of the relationship between distributed sources, feeders, and loads. The examples of the distributed generation sources are as follows: fuel cell, wind turbine, photovoltaic (PV), micro gas turbine, and low-power internal combustion turbine.

Wind turbines and PV panels are DG systems that are the most preferred. But in the recent period, micro gas turbines are often preferred for new applications due to its advantages over other sources such as small size, lightweight, and stable operation capability [1]. Different micro-cogeneration structures were observed when the literature is examined in detail. A novel PI control tuning technique is proposed to refrigerate the hydrogen generation part within the polymer electrolyte membrane fuel cell used in the micro-cogeneration system [2]. A dynamic simulation model of an Ericsson engine is presented for micro-cogeneration systems [3]. Another study in the literature, design, and effectiveness of a highly efficient micro-cogeneration system with a 20 kW prototype fueled by LNG or LPG is presented [4]. A survey and a comparison of basic national testing methods of micro-cogeneration are presented [5]. A sizing optimization procedure is proposed to increase the efficiency of a tubular linear induction generator for free-piston Stirling micro-cogeneration systems [6]. It is presented that the efficiency of micro-cogeneration system including single cylinder diesel engine with an experimental study [7]. Micro-cogeneration in low-energy buildings is proposed by using a load-sharing method. Simulations of two distinct areas in Italy are investigated for thermo-economic efficiency [8]. A micro-cogeneration Stirling unit is investigated for various conditions of the working fluid by experiment and simulation [9]. Efficiency and emission properties of a liquid fuel-fired vugular burner for micro-cogeneration of thermoelectric power are proposed by an experimental study [10]. An extensive literature survey of micro-cogeneration for facilities up to 100 kW consisting of working fluid imaging strategy, elements, expander choice, and detailed properties of industrial and experimental implementation is proposed [11]. Also, a combination of micro-cogeneration and electric vehicle charging systems is analyzed for two distinct areas in Italy with a parametric investigation in simulations [12].

The efficiency of micro-cogeneration systems is investigated with control techniques of Li-ion storage battery by simulations [13]. A high temperature PEM fuel cell based residential micro-cogeneration system is proposed and the detailed mathematical model of whole system is presented [14]. Investigation of the hybrid photovoltaic module-fuel cell combined with microgeneration implementations is presented. Efficiency forecast of the combined system is investigated for discrete climates in Ankara, Turkey [15]. Another fuel cell study, rural micro-cogeneration facility including a high-temperature proton-exchange membrane fuel cell with fuel partialization and power/heat shifting techniques, is presented [16]. A micro-cogeneration system with a solar parabolic collector and direct steam generation is investigated with a prototype [17].

The design model of a new solar micro-cogeneration system with Stirling machine is investigated in terms of efficiency and fuel pass analysis on TRNSYS simulation program for rural areas in Africa [18]. It is proposed that an auto-thermal membrane reformer is combined with a polymer electrolyte membrane fuel cell-based micro-cogeneration system on a prototype [19]. Modeling on TRNSYS simulation and validation by an experimental study of a micro-cogeneration system including an internal combustion engine is presented with over-temperature protection controls [20]. Thermal-economic optimization with generalized pattern search optimization method of a micro-cogeneration system consisting of a parabolic solar collector and Stirling engine is proposed in another micro-cogeneration structure [21].

Systems that use micro gas turbines are also known as micro-cogeneration systems. Micro-cogeneration systems are highly efficient and environment-friendly compared to other conventional energy sources shown in **Figure 1**, because they

produce second energy by using exhaust gases. Exhaust gases from the gas turbine are used in a waste heat boiler to obtain high-efficiency heat energy. Therefore, the waste heat is converted to usable energy in the micro-cogeneration system. Micro-cogeneration systems with gas engine also supply economical and eco-friendly concentrated heat and power. Eco-friendly micro-cogeneration power plants with combined heat and power enable economical and energy-efficient power production.

Cogeneration systems are 33% more efficient than coal that generates the same amount of heat and energy [22]. This paper analyzes the electrical modeling and performance investigation of a micro-cogeneration system in a microgrid to support renewables. This system comprises 30 kVA micro-cogeneration system, 10 kVA wind power station, 10 kVA photovoltaic power station, and local electrical loads. The system is designed by using real-time data. Firstly, PV and wind power station are modeled and simulated with the help of the system parameters. Then, a micro-cogeneration system suitable to the hybrid system has been designed by calculating the optimum efficiency.

Due to the limitations of the present studies in literature, the aim of this paper is:

- To demonstrate the mathematical model of the micro-cogeneration-based hybrid PV/wind energy system in detail.
- To test the performance analysis of the system, seven different scenarios are analyzed during the case studies firstly.
- To compare the case studies and investigate the performance.
- To get optimum performance for the implementation of the micro-cogeneration-based hybrid PV/wind energy system.

This paper primarily focuses on the aforesaid four aspects of the proposed system.

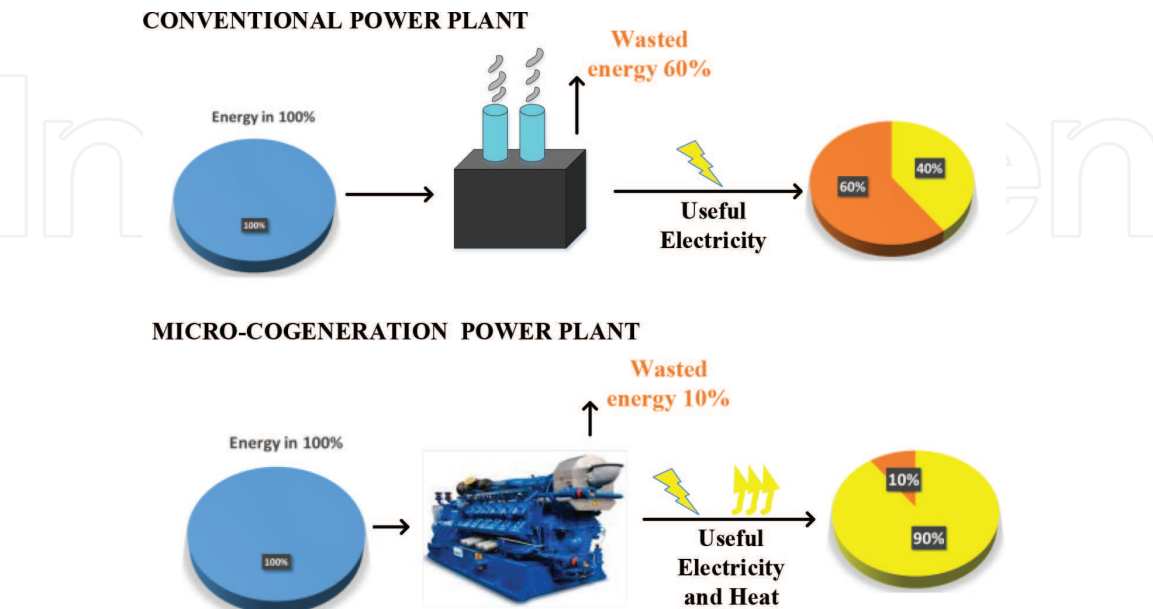


**Figure 1.**  
*Energy saving in micro-cogeneration power plant.*

## 2. Mathematical modeling and control of the proposed system

The proposed system consists of two parts: PV and wind system. These systems are examined in detail. The block diagram of the proposed system is shown in **Figure 2**. The control mechanism of **Figure 2** is explained in detail in the following section. The system consists of PV and wind power station, micro-cogeneration system, and the electrical grid. This integrated system feeds the dynamic electrical loads.

### 2.1 Mathematical modeling and control of micro-cogeneration system

Temperature control, speed control, fuel control, turbine dynamics, and acceleration control block are included in the micro-cogeneration system. The speed control provides to correct the speed error between the reference speed and the rotor speed of the permanent magnet generator system. It is the main control tool for microturbine under partial load conditions. Speed control modeling is done by using a lead-lag transfer function or by a PID controller [23]. Speed control for the micro-cogeneration system is shown in **Figure 3**.

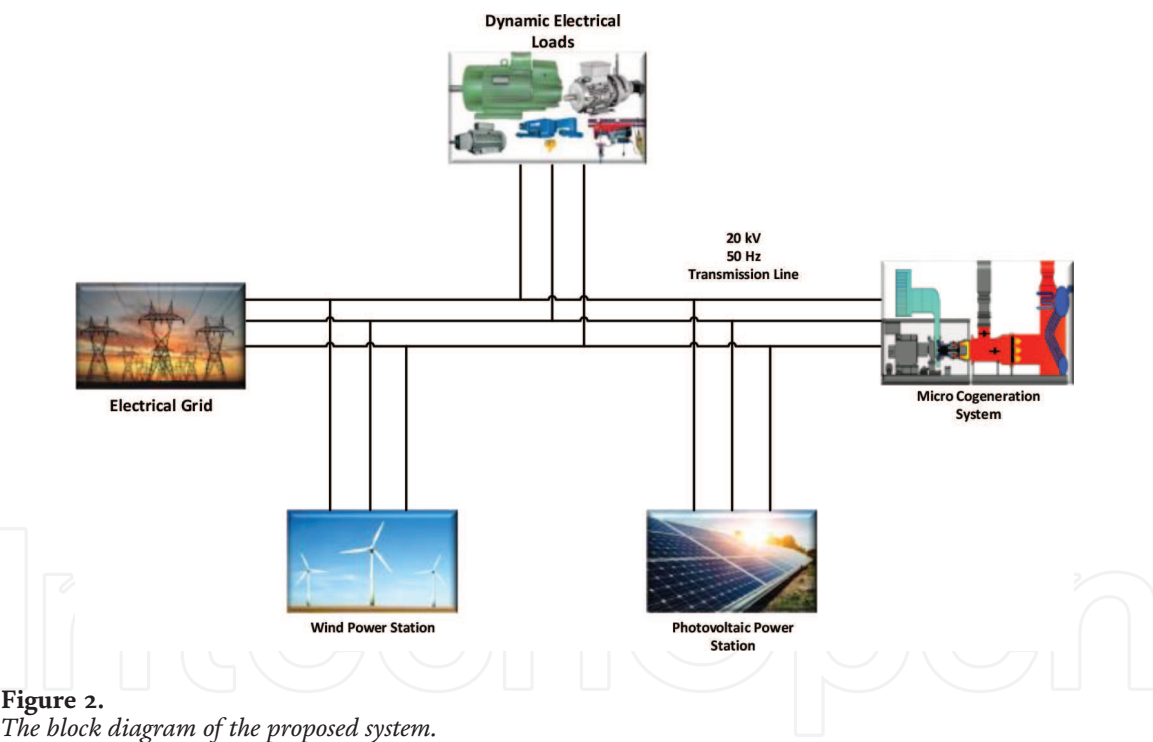


**Figure 2.**  
The block diagram of the proposed system.

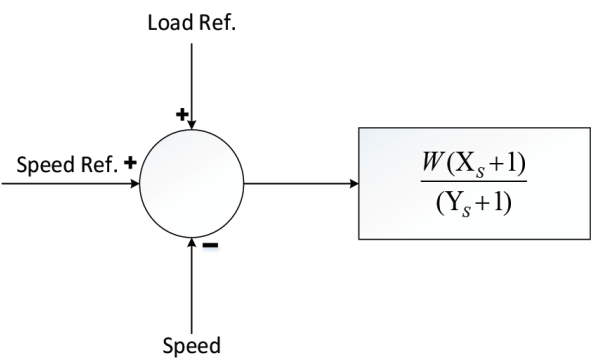


**Figure 3.**  
Speed control for the micro-cogeneration system.



W is the controller gain, X and Y are the governor lead and lag time constant, and Z is a constant representing the governor mode (droop or isochronous). X, Y, and Z can be adjusted so that the governor can act with droop or as an isochronous governor. Acceleration control allows limiting the rate of the rotor acceleration prior to reaching operating speed during turbine start-up. The fuel system consists of the fuel valve and actuator. The fuel system control is provided by the actuator and of the valve positioner shown in **Figure 4**.

$V_{ce}$  is the fuel flow control and the valve positioner transfer function is

$$E_1 = \frac{a}{(b_s + c)} \tag{1}$$

and the fuel system actuator transfer function is

$$E_2 = \frac{1}{(TF_s + 1)} \tag{2}$$

In Eq. (1) and (2), a is the valve positioner (fuel system actuator) gain, b and TF are the valve positioner and fuel system actuator time constants, c is a constant, E1 is the input and output of the valve positioner, and E2 is the fuel demand signal in pu.

Temperature control allows limiting the gas turbine output power at a predetermined firing temperature, independent of variation in ambient temperature or fuel characteristics. The fuel burned in the burner causes the movement of the turbine (torque) and the exhaust gas temperature. The exhaust temperature is measured using a series of thermocouples incorporating radiation shields as shown in **Figure 5** [24].

0.8 and 0.2 values are constants associated with the radiation shield, and 3.3 value is the time constant associated with a temperature controller. TT is the temperature controller integration rate, and 15 and 2.5 values are time constants associated with the radiation shield and thermocouple, respectively.

Permanent magnet generators are superior alternatives to conventional induction motors that can be combined with turbines. The main advantages of PMSG are considerably significant: higher operational reliability, higher

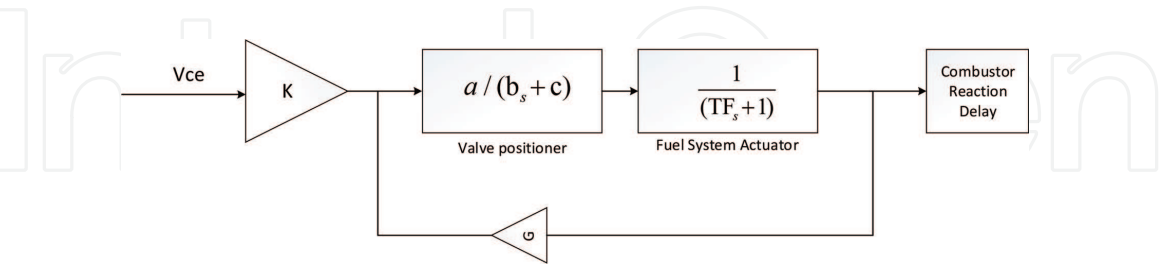


**Figure 4.**  
Fuel system control for the micro-cogeneration system.

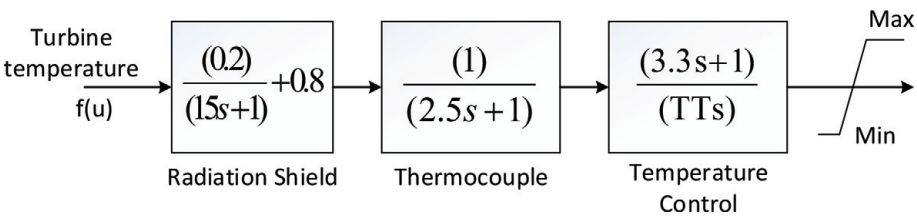


**Figure 5.**  
Temperature controller.

efficiency, and very small energy loss. The microturbine generates electrical energy through a high-speed permanent magnet generator driven directly by the turbo compressor shaft. Totally, 30 kVA electricity is produced by the proposed micro-cogeneration system. The model adopted for the generator is a 2-pole permanent magnet machine generator with a non-salient rotor. At 50 hertz (3000 rpm), the machine output power is 30 kW, and its terminal line-to-line voltage is 380 V.

$\omega$  (in pu) is angular velocity,  $m$  is speed signal, and  $P_m$  is specified as shaft mechanical torque value shown in **Figure 6**.

The electrical and mechanical equations of permanent magnet machine expressed in rotor reference frame dq are as follows [25]:

Electrical equations:

$$\frac{d}{dt}i_d = \frac{1}{L_d}v_d - \frac{R}{L_d}i_d + \frac{L_q}{L_d}p\omega_r i_q \quad (3)$$

$$\frac{d}{dt}i_q = \frac{1}{L_q}v_q - \frac{R}{L_q}i_q - \frac{L_d}{L_q}p\omega_r i_d - \frac{\lambda p\omega_r}{L_q} \quad (4)$$

$$T_e = 1.5p(\lambda i_q + (L_d - L_q)i_d i_q) \quad (5)$$

Mechanical equations:

$$\frac{d}{dt}\omega_r = \frac{1}{J}(T_e - F\omega_r - T_M) \quad (6)$$

$$\frac{d\theta}{dt} = \omega_r \quad (7)$$

## 2.2 Mathematical modeling and control of PV system

PV power plant is modeled by using five parallel strings and six series-connected modules per string in order to obtain 10 kWp solar PV power. Solar PV module data is indicated in **Table 1**.

One basic solar cell equivalent circuit model in common use is the single-diode model, which is derived from physical principles. The equivalent circuit of a solar PV cell can be represented with a current source which is connected parallel with a diode as shown in **Figure 7** [26].

This equivalent circuit is formulated using Kirchhoff's current law for current:

$$I = I_g - I_d - I_{sh} \quad (8)$$

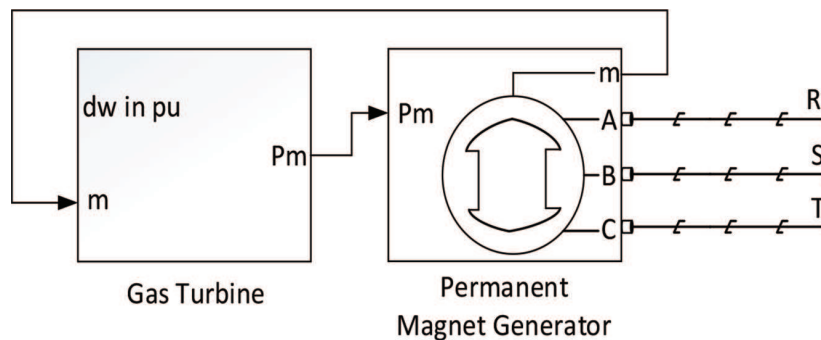


**Figure 6.**  
Permanent magnet generator model implemented in SimPowerSystems.

Maximum power (W)	414.801	Cells per module (Ncell)	128
Open circuit voltage Voc (V)	85.3	Short-circuit current Isc (A)	6.09
The voltage at maximum power point Vmp (V)	72.9	Current at maximum power point Imp (A)	5.69

**Table 1.**  
*PV module parameters.*

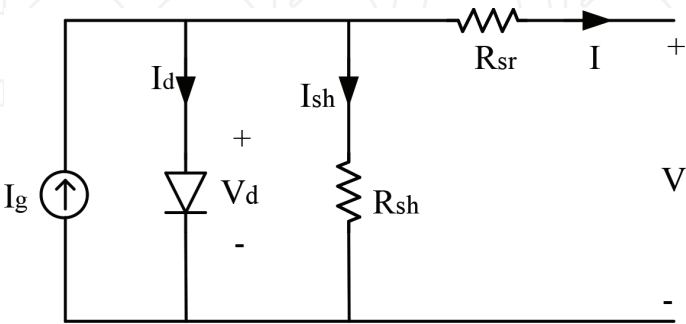


**Figure 7.**  
*Equivalent circuit of solar PV cell.*

where  $I_g$  represents the light-generated current in the cell,  $I_d$  represents the voltage-dependent current lost to recombination, and  $I_{sh}$  represents the current loss due to shunt resistances. The substitution of the related expressions for the diode current  $I_d$  and the shunt branch current  $I_{sh}$  is given in Eq. (4):

$$I = I_g - I_0 \left[ \exp \left( \frac{V + IR_{sr}}{nkT_c/q} \right) - 1 \right] - \left( \frac{V + IR_{sr}}{R_{sh}} \right) \tag{9}$$

where  $n$  is the diode ideality,  $I_0$  is the saturation current,  $k$  is Boltzmann's constant ( $1.381 \times 10^{-23}$  J/K), and  $q$  is the elementary charge ( $1.602 \times 10^{-19}$ C). A group of single cells can be connected either series or parallel combination. By connecting solar cells, PV module can be created. Similarly, by connecting PV modules, a PV array can be created. Power calculation of a solar PV cell is obtained by the equation:

$$P_{pv(t)} = V \times I \tag{10}$$

where  $P_{pv(t)}$  is solar PV cell DC power,  $V$  is solar cell or PV array voltage, and  $I$  is current flowing from solar PV cell.

If the generated power on the PV module does not match the load power, there will be an efficiency loss. To overcome this problem, a PV panel must operate at its maximum power point. The variations in solar radiation and temperature affect the maximum power point. In order to prevent losses due to operating point, a maximum power point tracker should be used in PV power systems. For the proposed system Perturb and Observe (P&O) algorithm is used to track the maximum power point. The purpose of the algorithm is to find VMPP and IMPP points that PV system delivers the maximum point. The algorithm is based on a periodic increase and decrease in PV voltage. After an increase/decrease, the system checks the output power. According to the tendency of the output power, the tracker decides if the next voltage perturbation will be in the same way or the opposite way [27]. The flowchart of the P&O algorithm is shown in **Figure 8**.



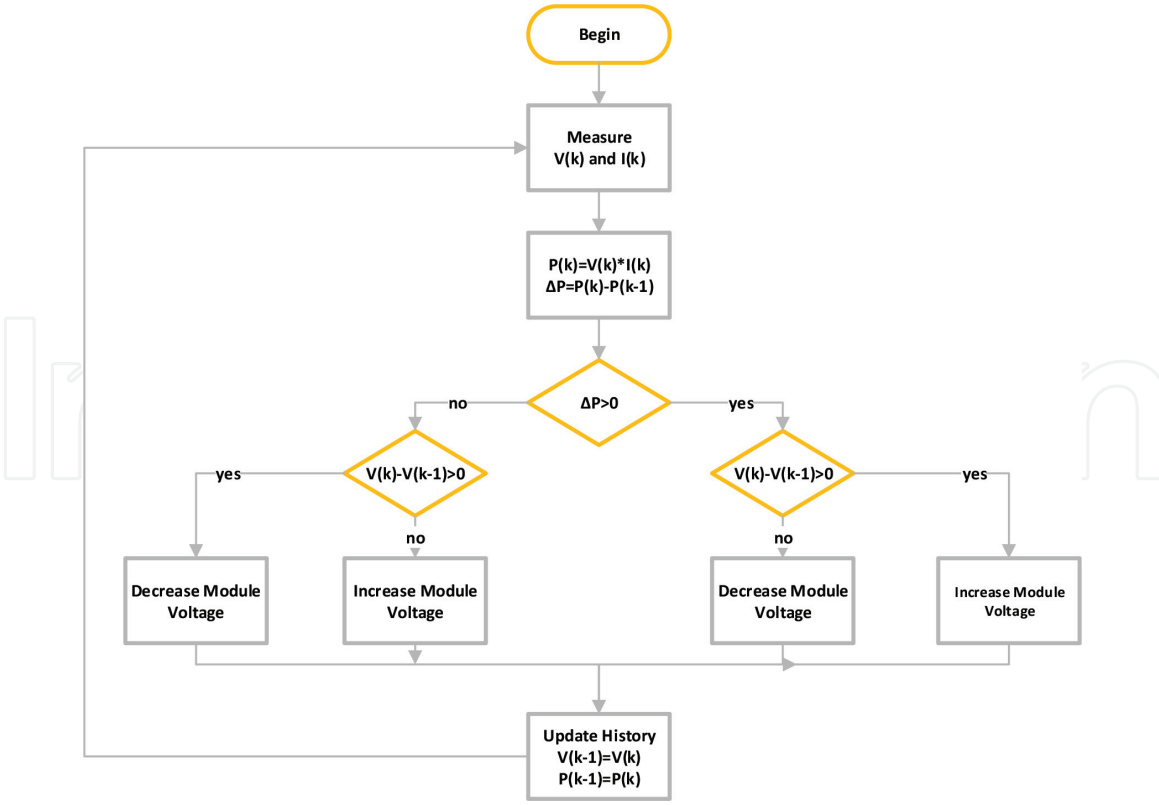


**Figure 8.**  
The flowchart of the P&O algorithm [28].

### 2.3 Mathematical modeling and control of wind energy conversion system

The proposed wind turbine consists of a rotor mounted to a nacelle and a tower with two or more blades mechanically connected to a wind turbine electric generator. Wind passes over the blades of the wind turbine. Wind power extracted from wind is expressed in Eq. (6) [29]:

$$P_m = \frac{1}{2} \cdot C_p(\lambda, \beta) \cdot \rho \cdot A \cdot v^3 \quad (11)$$

where  $C_p(\lambda, \beta)$  is the power coefficient,  $\lambda$  is named as tip speed,  $\beta$  (degree) is the pitch angle of the rotor blades,  $A$  is swept area ( $\pi r^2$ ),  $\rho$  is air density ( $1.25 \text{ kgm}^3$ ), and  $v$  is named wind speed (m/sn).

The rotating blades turn a shaft that goes into a gearbox in nacelle. The blades of the wind turbine create kinetic energy given Eq. (7):

$$E = 0.5 \text{ } mv^2 \quad (12)$$

where  $m$  is the air mass and  $v$  is the wind speed. Air power is obtained by the time derivative of kinetic energy. Air power is given in the following equation:

$$P_w = \frac{d(0,5.m.v^2)}{dt} \quad (13)$$

where  $m$  is the mass flow rate per second and air power is obtained from Eq. (9):

$$P_w = 0,5.m.\rho.A.v^2 \quad (14)$$

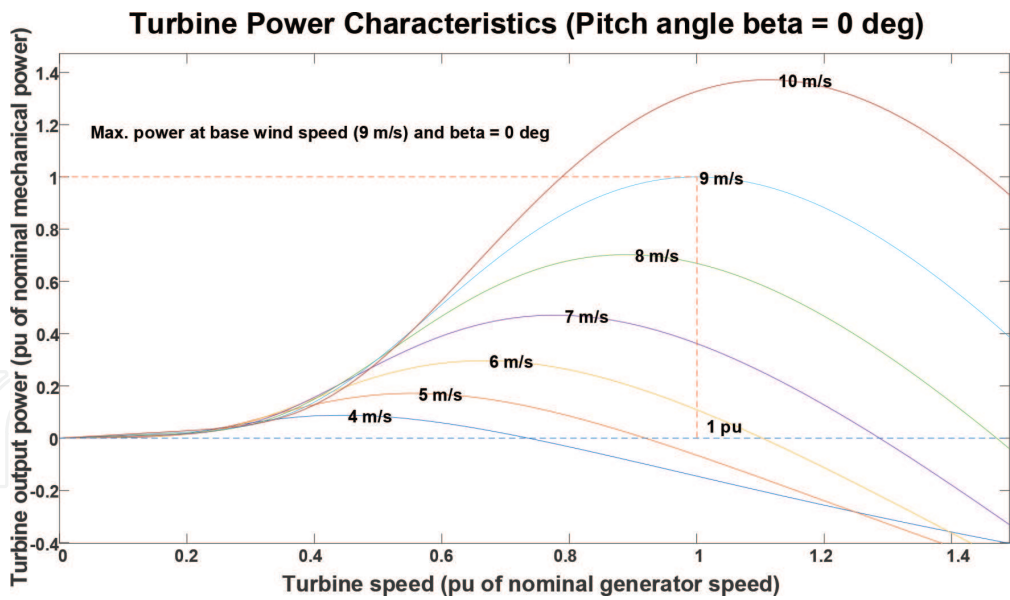


Figure 9.  
Power characteristics of the wind turbine.

Blade power resulted by wind effect is given by Eq. (10):

$$P_{blade} = C_p(\lambda, \beta) \cdot 0.5 \cdot \rho \cdot A \cdot v^3 \tag{15}$$

Tip speed and rotor torque theoretical parameters are given in Eqs. (11) and (12):

$$\lambda = \frac{w_m \cdot R}{v} \tag{16}$$

$$T_{wr} = \frac{P_{blade}}{w_m} = \frac{C_p(\lambda, \beta) \cdot \rho \cdot A \cdot v^3}{2 \cdot w_m} \tag{17}$$

where  $T_{wr}$  is the rotor torque and  $w_m$  is the angular velocity of the rotor.

The gearbox in the mechanical assembly named as drive train mechanism provides to transform slower rotational speeds of the wind turbine to higher rotational speeds on the wind turbine electric generator. The rotation of the electric generator's shaft generates wind turbine power.

The power coefficient of the wind turbine, therefore, the generated power can be controlled by changing the pitch angle ( $\beta$ ). **Figure 9** shows that as the wind

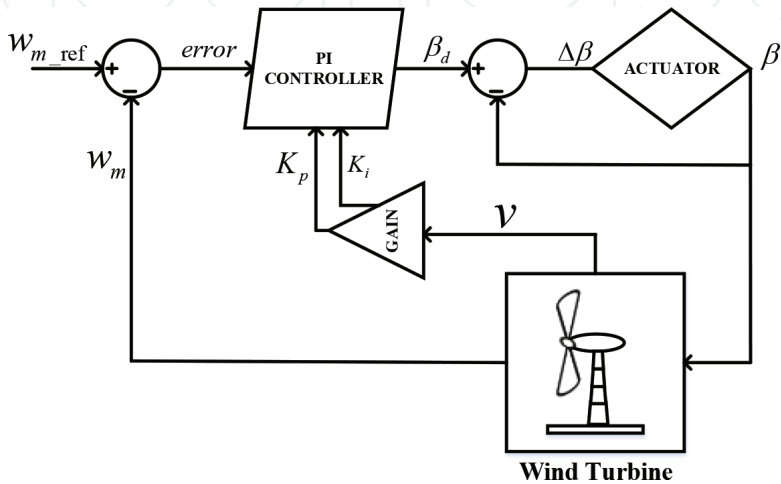


Figure 10.  
Block diagram of pitch angle PI controller [31].

speed increases, the amount of power generated by the turbine also increases. According to Eq. (11), further increase in wind speed will result in a further increase in turbine power. But this will also bring a random surge of power. In order to prevent this condition, a control system must keep the power at a constant level. PI controller is used for this purpose in the proposed system [30].

**Figure 10** shows the block diagram of the pitch angle PI controller. The pitch angle controller checks the speed and compares it with a reference speed. If the speed is greater than the reference speed, the controller changes the pitch angle in order to approach the rated speed [31].

### 3. Performance analysis of proposed system and controllers

In this section, the performance evaluation of the proposed system and controllers will be evaluated. The proposed system is modeled using MATLAB/SIMULINK. To test the performance of the system, seven different simulation scenarios are created. In the simulation study, parameters such as wind speed, solar radiation, temperature, and electrical load demand are changed and the resulting graphs of active power, voltage, and currents for each element were taken. The summary of the scenarios can be seen in **Table 2**.

#### 3.1 Case 1

In this case, the parameters such as wind speed, solar radiation, temperature, electrical load demand and the fuel flow of the micro gas turbine are assumed steady during simulation time. The active power flow in the proposed system can be seen in **Figure 11**.

#### 3.2 Case 2

In this case, only solar radiation and temperature on the PV module are variable. This variation affects the output power of the PV station, hence, the grid power. The resulting active power can be seen in **Figure 12**. RMS voltages and currents of the grid and the PV station can be seen from **Figures 13** and **14**, respectively; **Figure 15** shows solar radiation and temperature during simulation of this case.

In this scenario, it is observed that the variations in solar radiation and temperature make the output power of the PV plant variable. Hence, the balance in case 1 is no longer observable. The missing power is supplied by the electrical grid.

Cases	PV system	WECS	Load	Micro-cogeneration system
Case 1	Steady	Steady	Steady	Steady
Case 2	Variable	Steady	Steady	Steady
Case 3	Variable	Variable	Steady	Steady
Case 4	Variable	Steady	Variable	Steady
Case 5	Steady	Variable	Variable	Steady
Case 6	Steady	Steady	Variable	Steady
Case 7	Variable	Variable	Variable	Steady

**Table 2.**  
*The summary of the scenarios.*

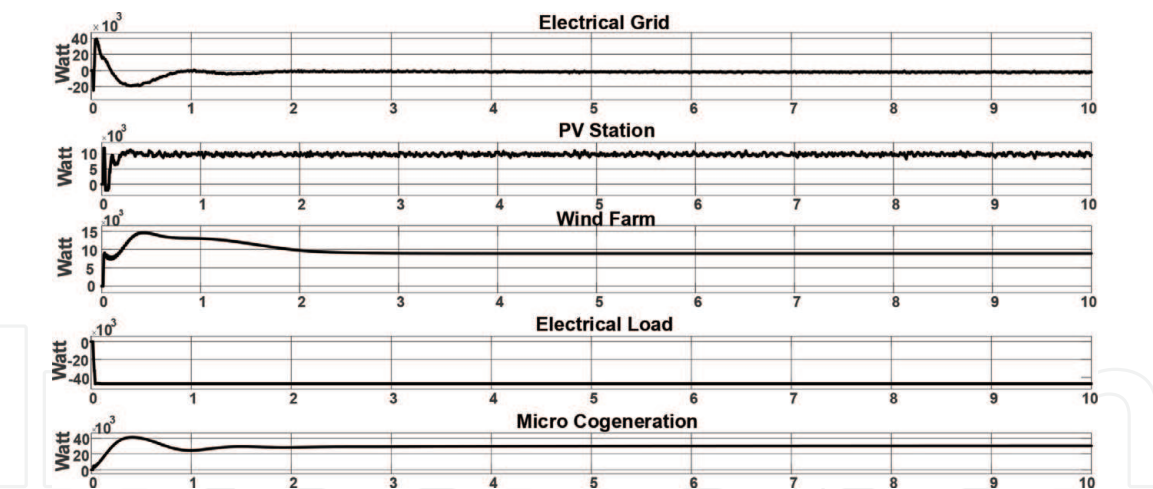


**Figure 11.**  
The graph of active power of the elements in proposed system for case 1 (wind speed 10 m/s, solar irradiance 1000 W/m<sup>2</sup>, temperature 25°C).

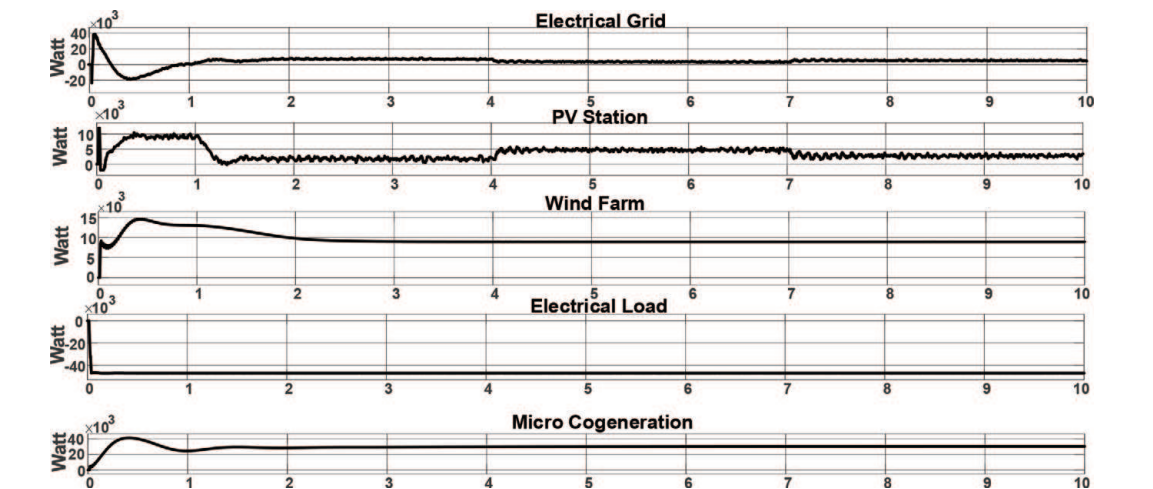


**Figure 12.**  
The graph of active power of the elements in proposed system for case 2 (wind speed is 10 m/s).

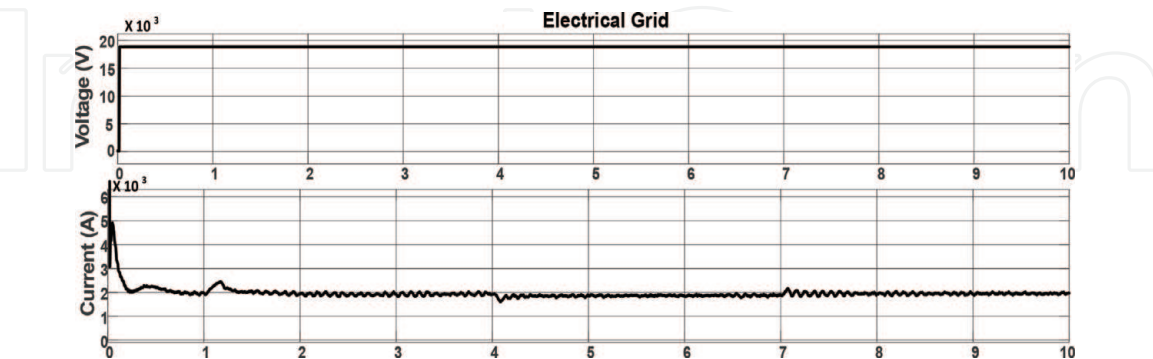


**Figure 13.**  
RMS voltage and RMS current of electrical grid for case 2.

### 3.3 Case 3

In this case wind speed, solar radiation, and temperature are variable. This variation affects the output power of the wind farm and PV station and the power fed to the electrical grid. The resulting active power graph can be seen in **Figure 16**. RMS voltages and currents of the electrical grid, PV station, and wind farm can be

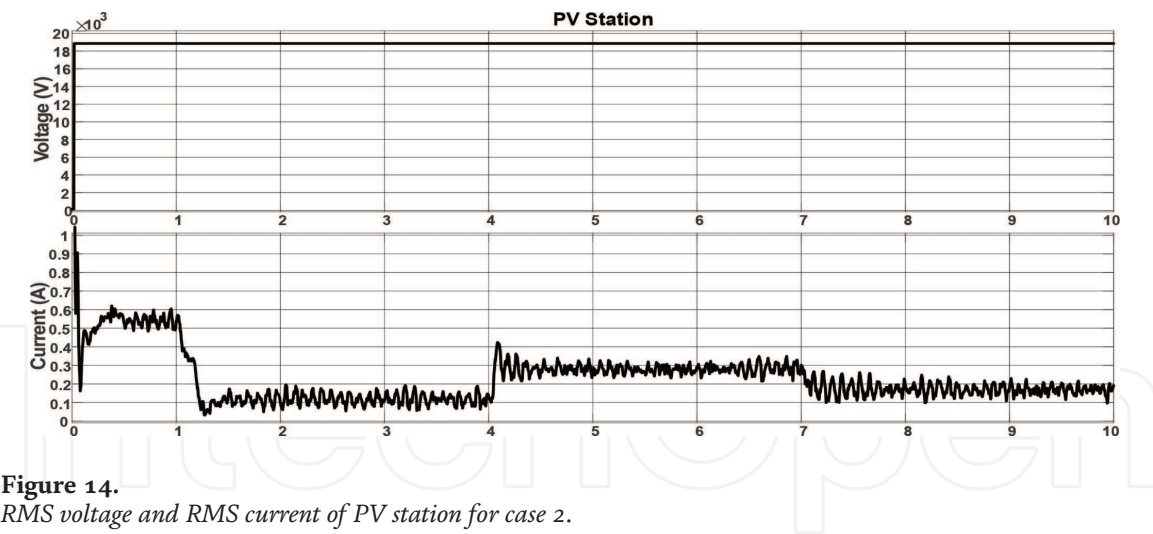


Figure 14.  
RMS voltage and RMS current of PV station for case 2.

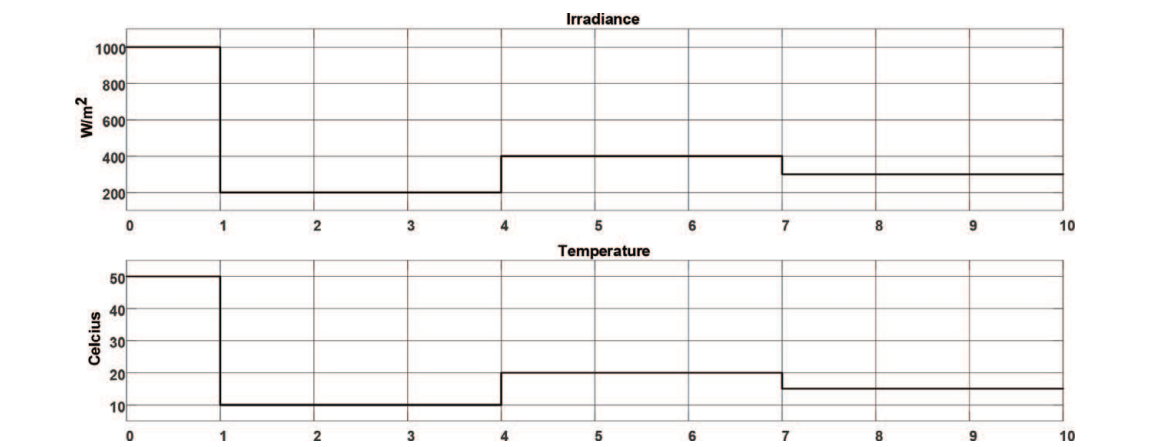


Figure 15.  
Graph of solar radiation and temperature for case 2.

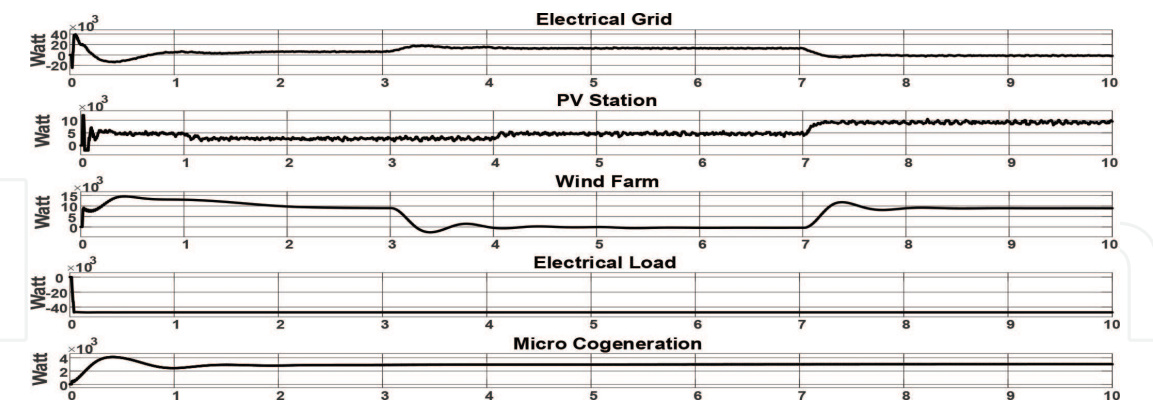


Figure 16.  
The graph of active power of the elements in proposed system for case 3 (wind speed is 10 m/s).

seen from **Figures 17–19**. The graph of wind speed, solar radiation, and temperature can be seen from **Figures 20 and 21**.

In this scenario in addition to case 2, the wind speed was also variable. The missing power is supplied by the electrical grid. Variations in wind speed caused better observability of variations in grid power.

3.4 Case 4

In this case, electrical load demand, solar radiation, and temperature are variable. This variation affects the output power PV station and the power fed to/from



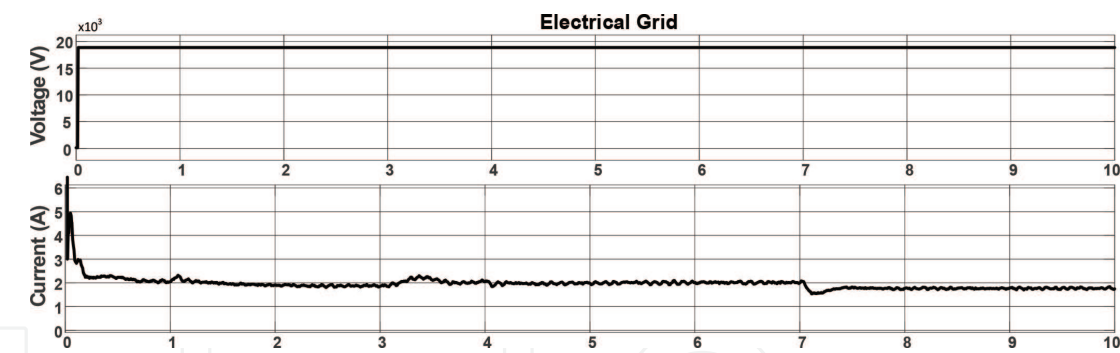


**Figure 17.**  
RMS voltage and RMS current of electrical grid for case 3.

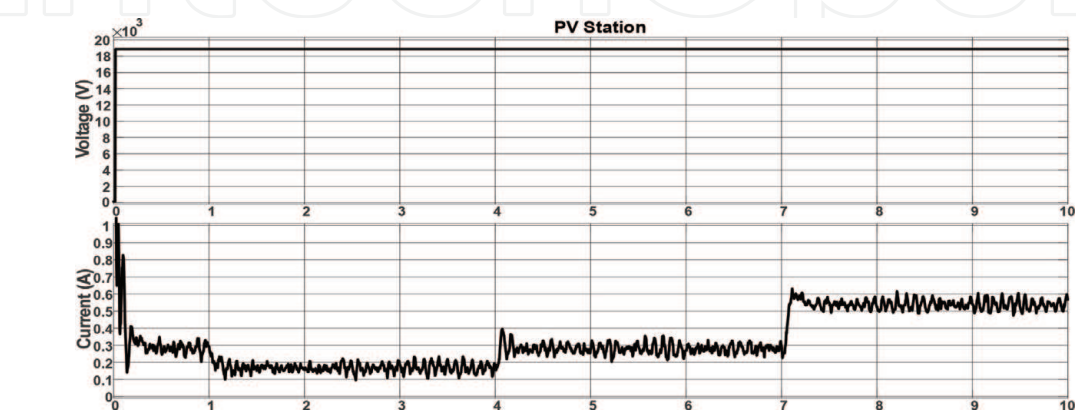


**Figure 18.**  
RMS voltage and RMS current of PV station for case 3.

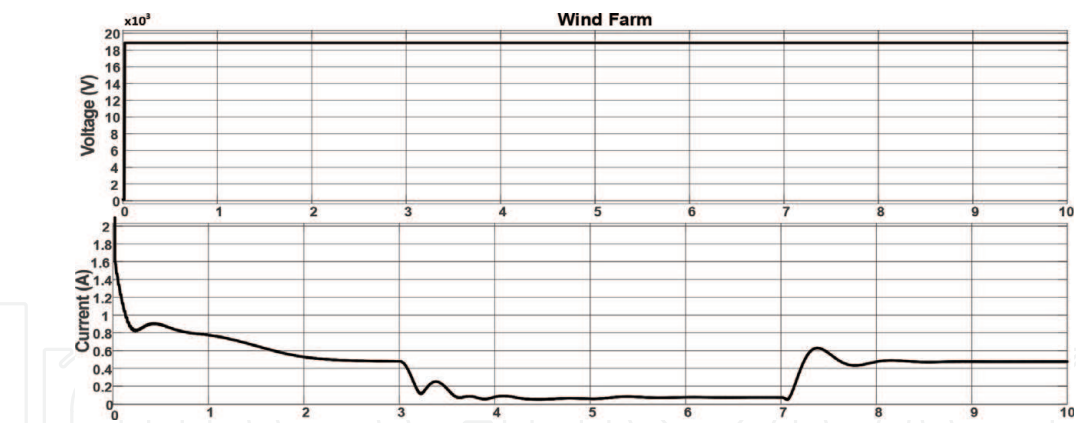


**Figure 19.**  
RMS voltage and RMS current of wind farm for case 3.

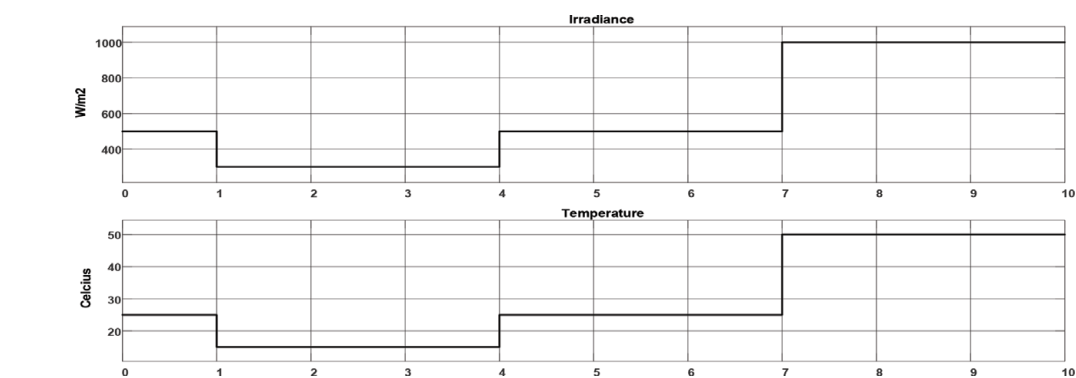


**Figure 20.**  
Graph of solar radiation and temperature for case 3.

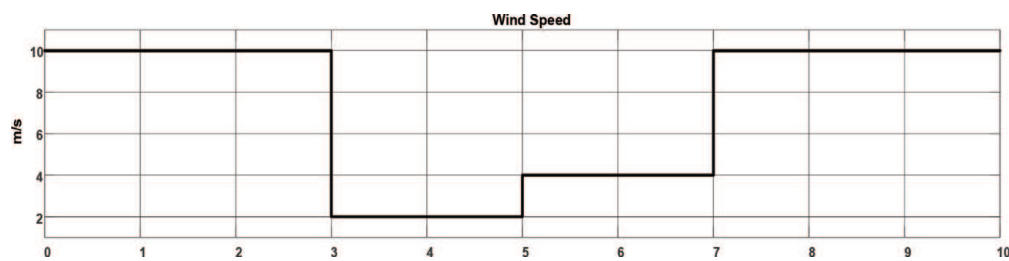


Figure 21.  
Graph of wind speed for case 3.

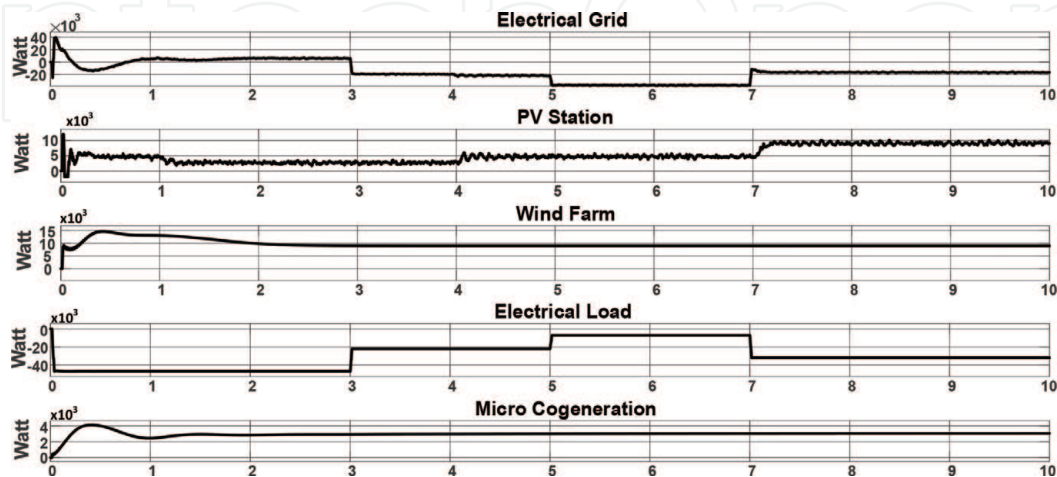


Figure 22.  
The graph of active power of the elements in proposed system for case 4.

the electrical grid. The resulting active power graph can be seen in **Figure 22**. RMS voltages and currents of the electrical grid, PV station, and electrical load can be seen from **Figures 23–25**. The graph of solar radiation and temperature can be seen in **Figure 26**.

In this scenario in addition to solar radiation and temperature, load demand was also variable. It is observed that when load demand decreases, the excessive power is supplied to the electrical grid.

### 3.5 Case 5

In this case, the electrical load demand and wind speed are variable. This variation affects the output power wind farm and the power fed to the electrical grid. The resulting active power graph can be seen in **Figure 27**. RMS voltages and

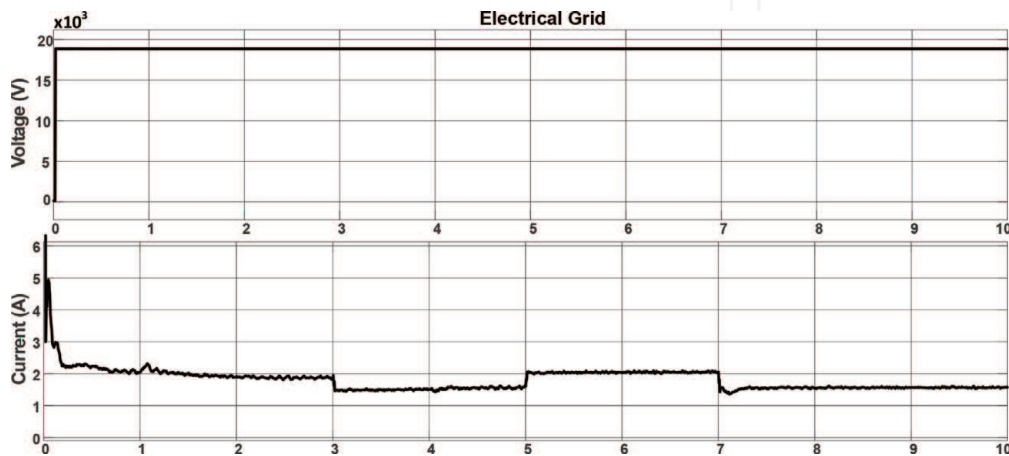


Figure 23.  
RMS voltage and RMS current of electrical grid for case 4.

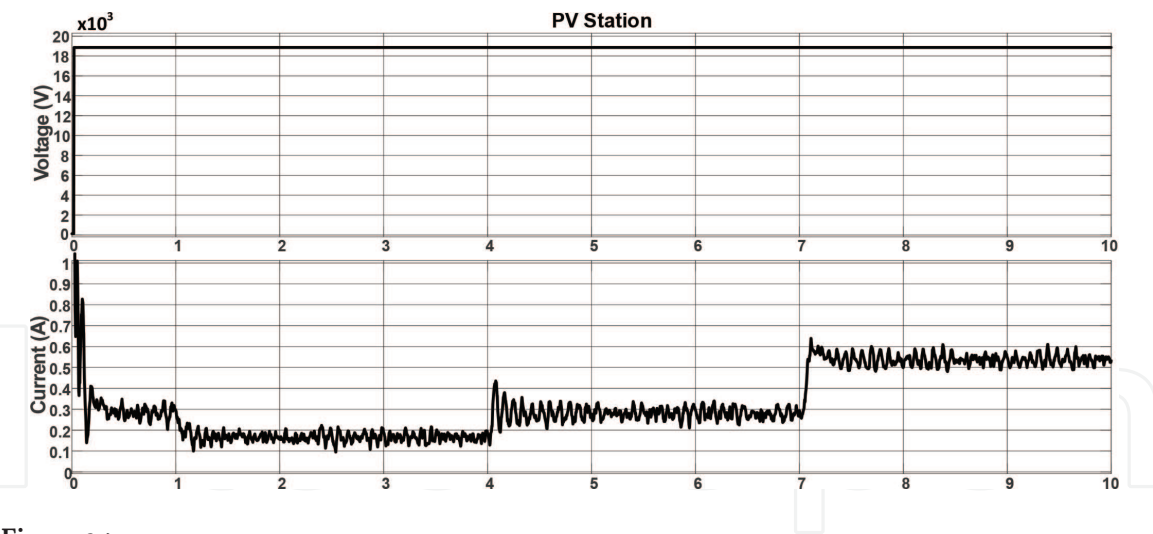


Figure 24.  
RMS voltage and RMS current of PV station for case 4.

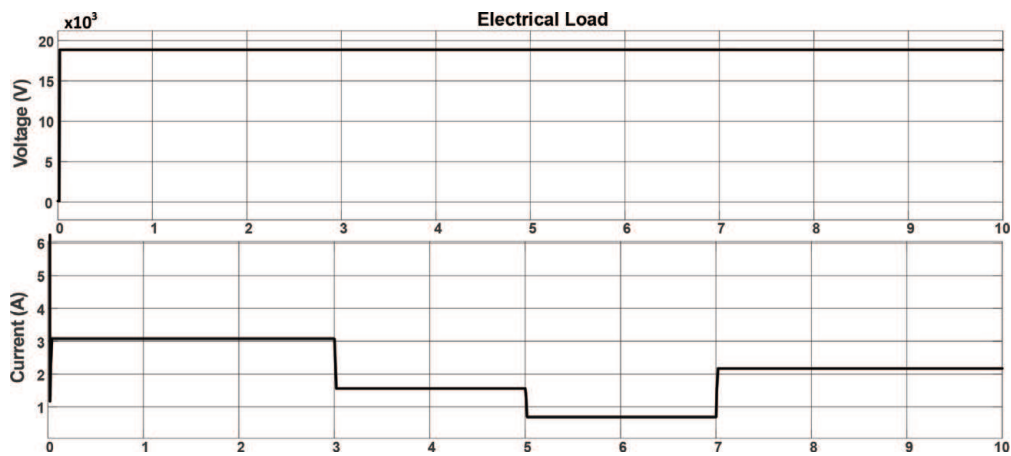


Figure 25.  
RMS voltage and RMS current of electrical load for case 4.

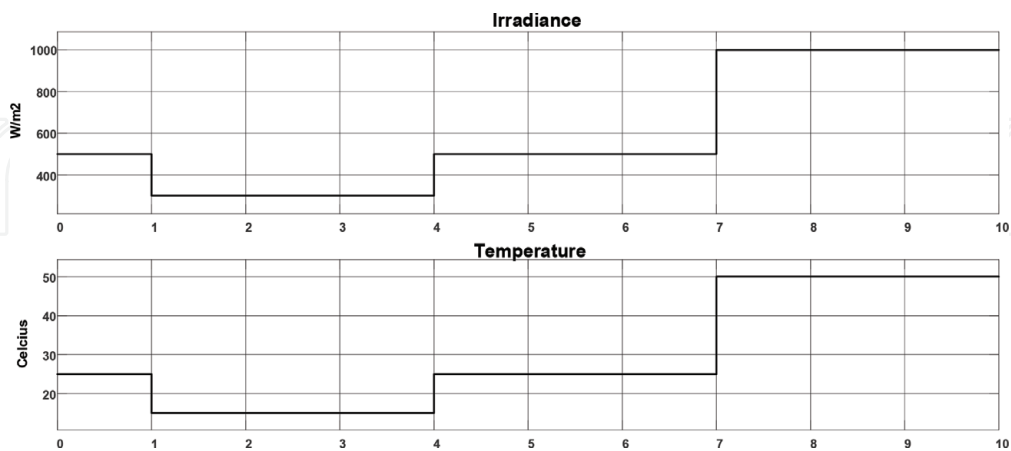


Figure 26.  
Graph of solar radiation and temperature for case 4 (wind speed 10 m/s).

currents of the electrical grid, wind farm, and electrical load can be seen from **Figures 28–30**. The graph of wind speed can be seen in **Figure 31**.

In this scenario, the wind power generation and the load demand were variable. It is observed that when the wind power generation is decreased and the load demand is increased, the excessive load demand is supplied from the electrical grid.

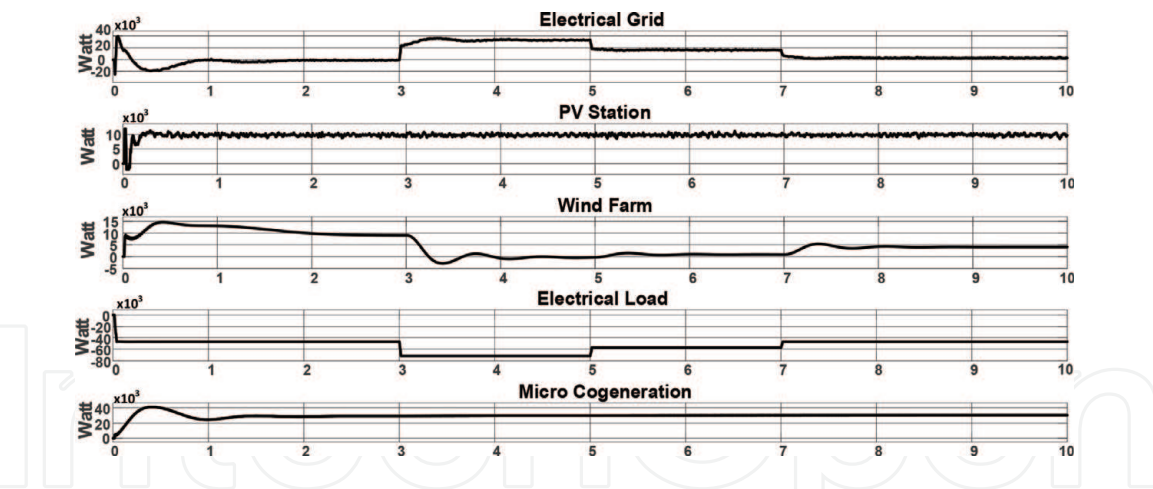


Figure 27.  
The graph of active power of the elements in proposed system for case 5.

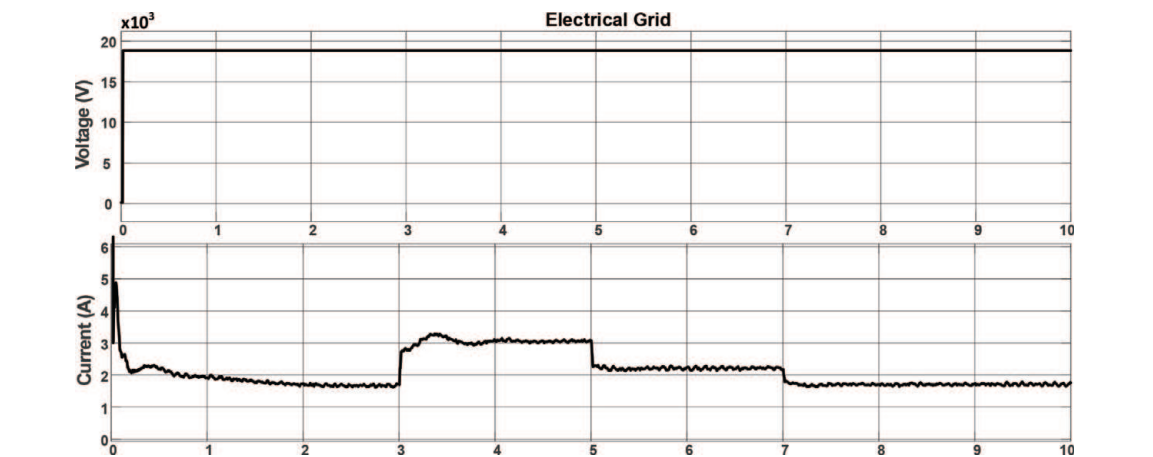


Figure 28.  
RMS voltage and RMS current of electrical grid for case 5.

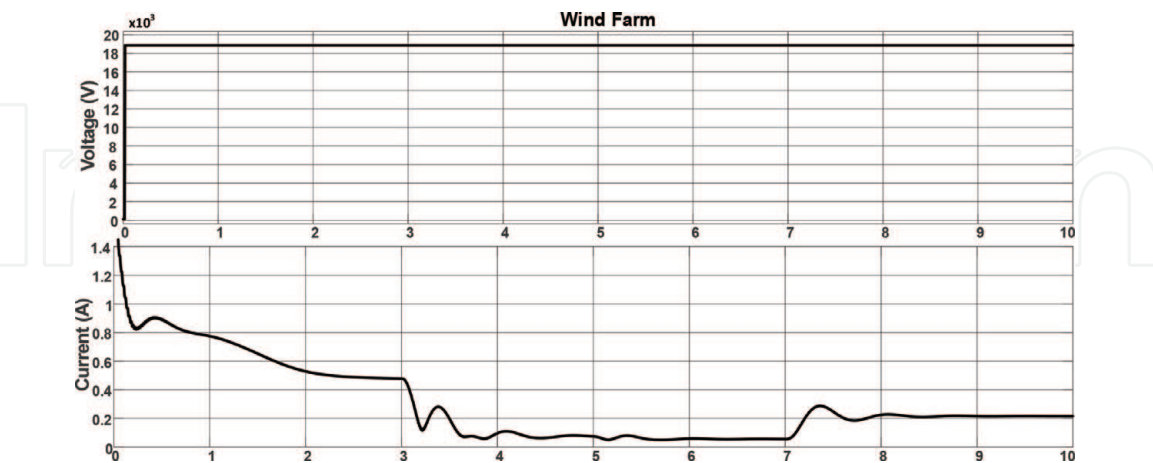


Figure 29.  
RMS voltage and RMS current of wind farm for case 5.

### 3.6 Case 6

In this case, electrical load demand is variable. This variation affects the power fed to the electrical grid. The resulting active power graph can be seen in **Figure 32**. RMS voltages and currents of the electrical grid and electrical load can be seen from **Figures 33 and 34**.

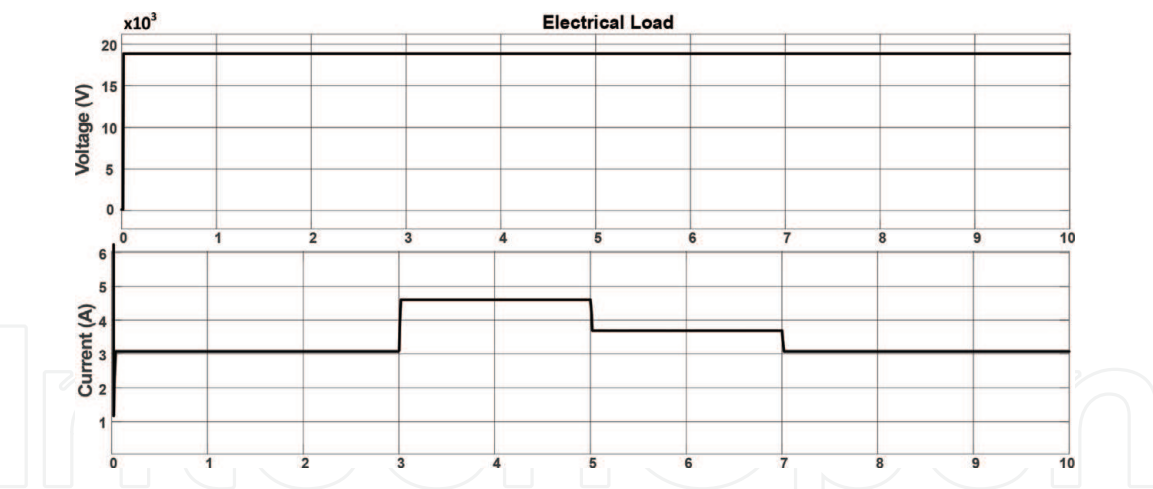


Figure 30.  
RMS voltage and RMS current of electrical load for case 5.

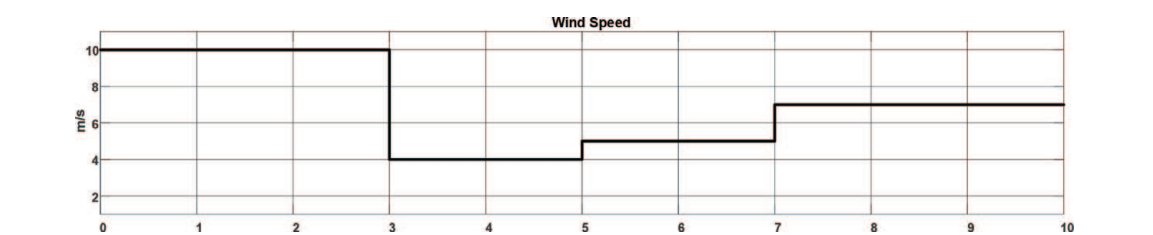


Figure 31.  
Graph of wind speed for case 5.

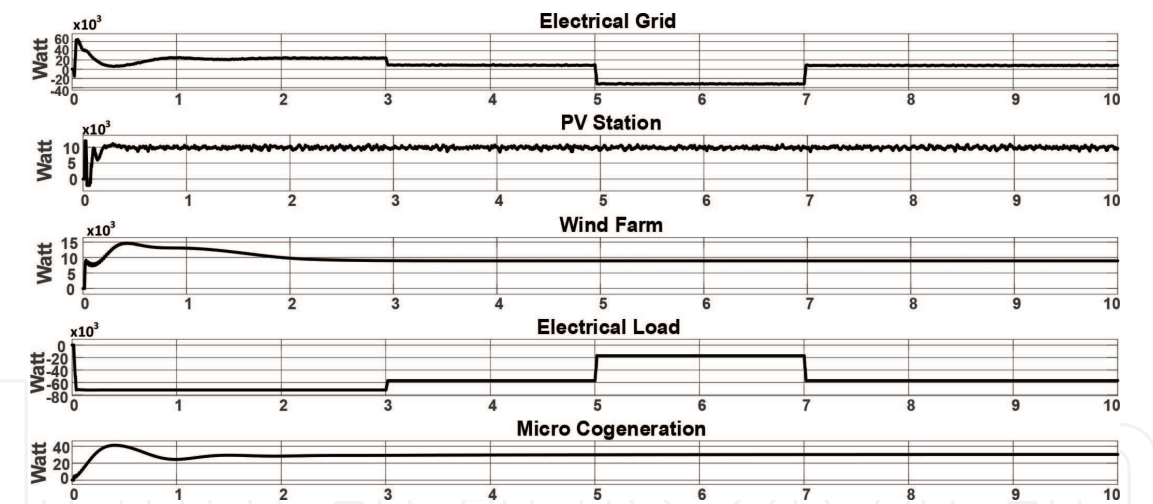


Figure 32.  
The graph of active power of the elements in proposed system for case 6.

In this scenario, the only variable parameter was load demand, and both the supply of loads from the electrical grid and the transfer of excess power to the electrical grid have been observed. It is seen that the variations in load demand caused the same amount but reversed variation in the grid power.

### 3.7 Case 7

In this case, the electrical load demand, wind speed, solar radiation, and temperature are variable. This variation affects the output power of a wind farm, PV station, and the power fed to the electrical grid. The resulting active power graphs can be seen in **Figure 35**. RMS voltages and currents of all the elements can be seen



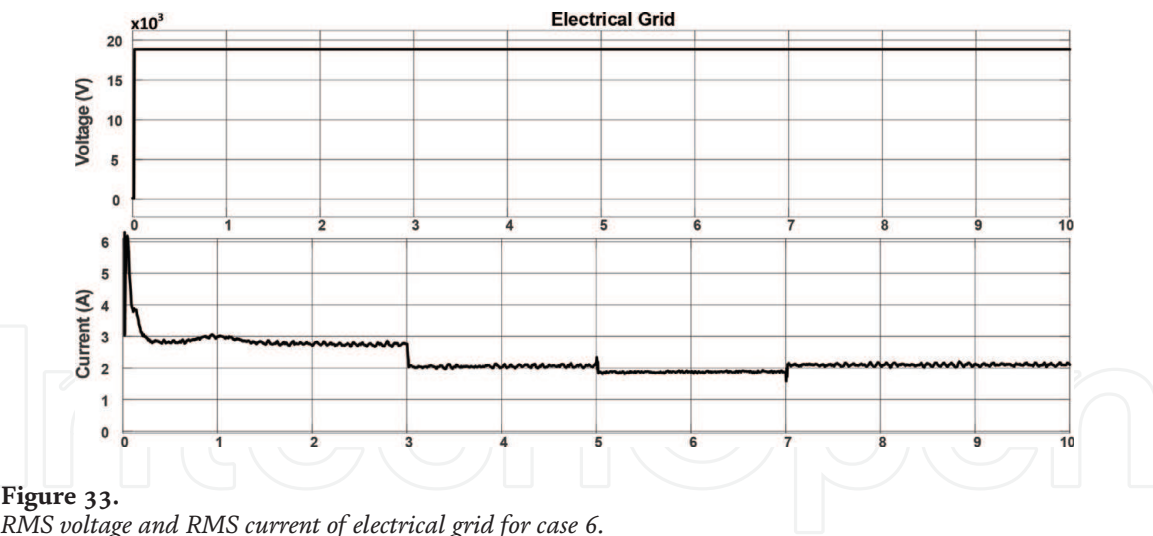


Figure 33.  
RMS voltage and RMS current of electrical grid for case 6.

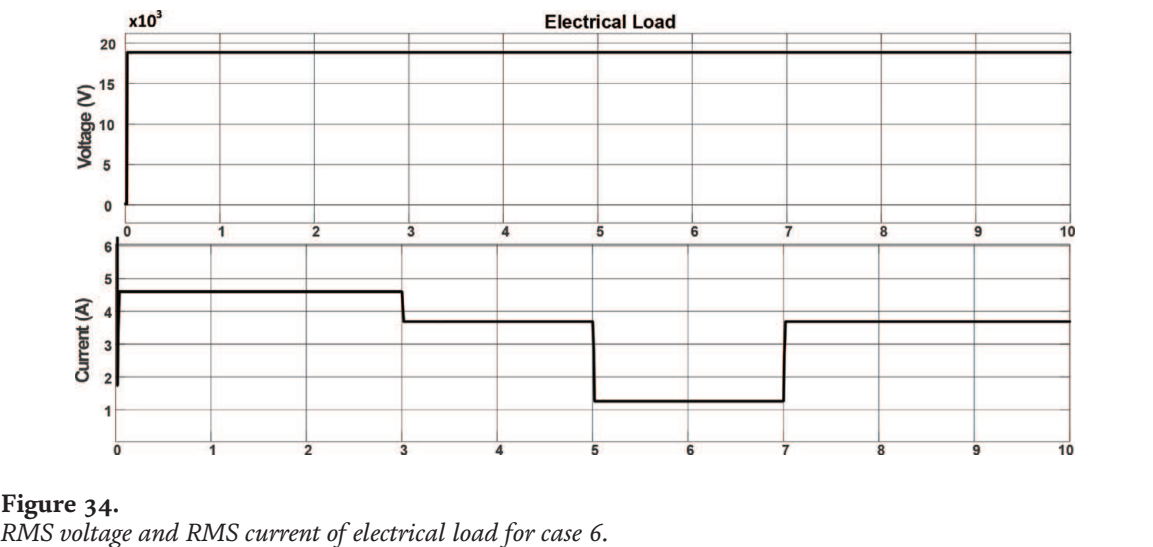


Figure 34.  
RMS voltage and RMS current of electrical load for case 6.

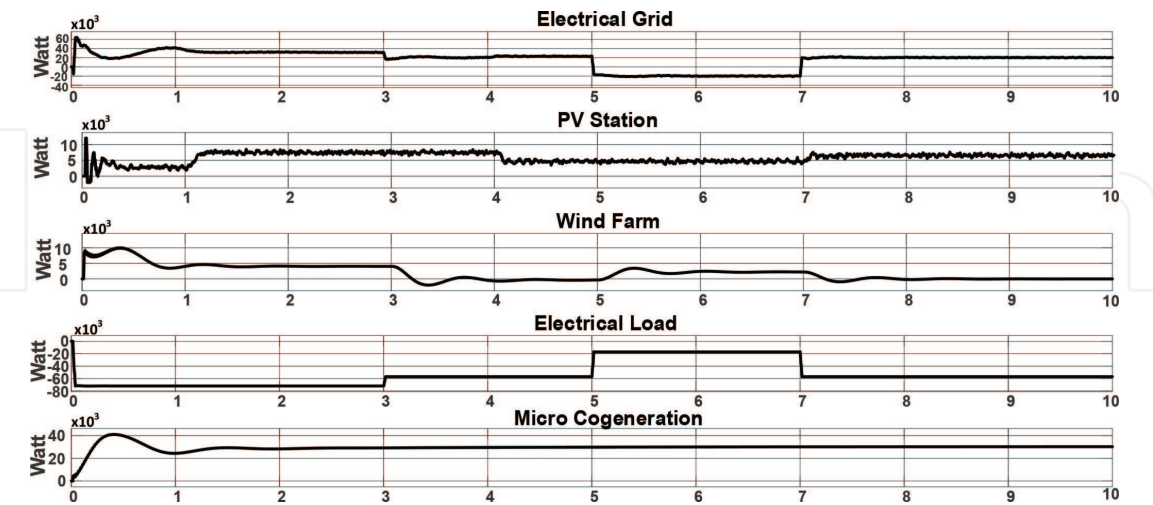


Figure 35.  
The graph of active power of the elements in proposed system for case 7.

from **Figures 36–39**. The graph of wind speed, solar radiation, and temperature can be seen from **Figures 40 and 41**.

In this scenario wind speed, load demand, solar radiation, and temperature were variable. It is observed that despite the output power variations of the PV plant and WECS because of these variations, the system did not go to an unstable state.

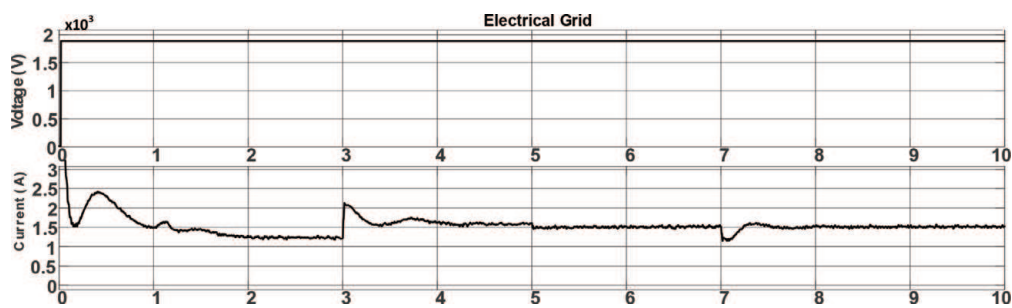


Figure 36.  
RMS voltage and RMS current of electrical grid for case 7.

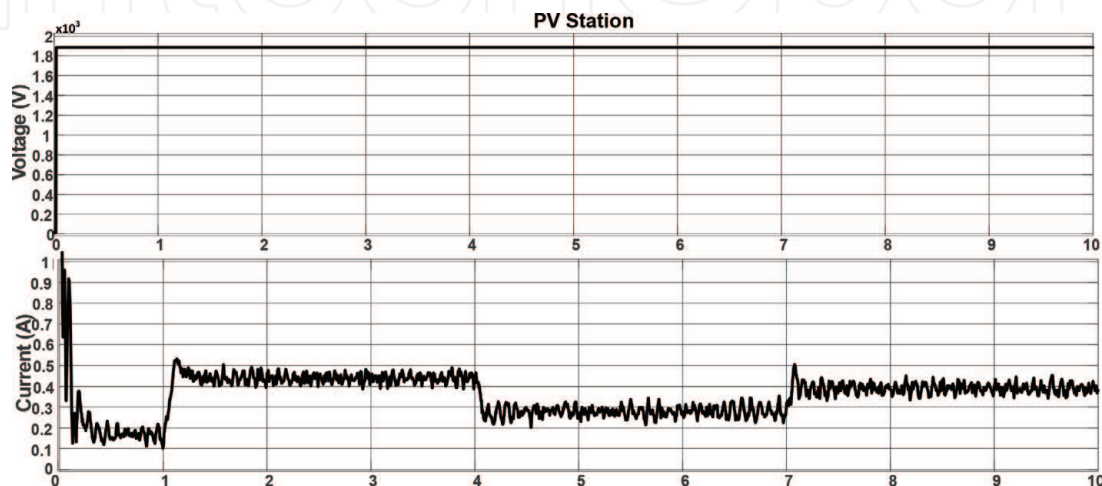


Figure 37.  
RMS voltage and RMS current of PV station for case 7.

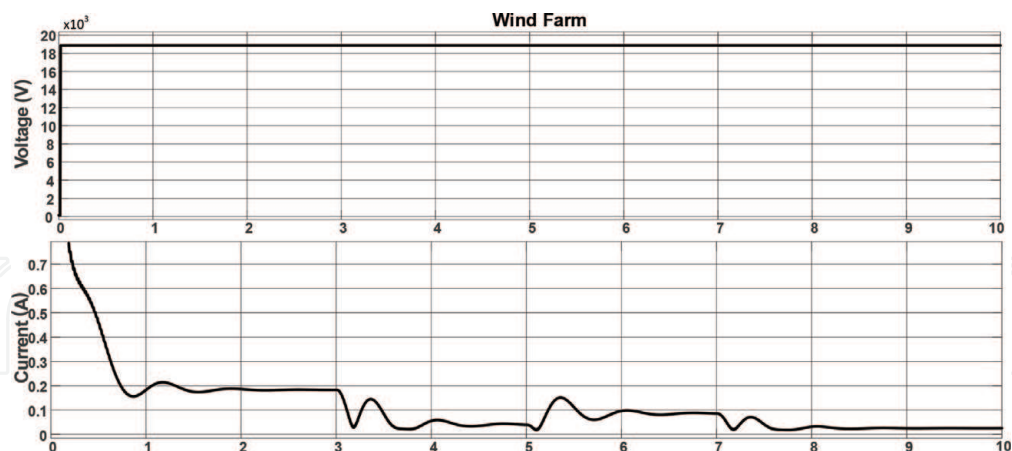


Figure 38.  
RMS voltage and RMS current of wind farm for case 7.

**Table 3** summarizes the power generation/consumption of the elements of the proposed system during simulations of the specified scenarios. Minus sign means power consumption; plus sign means power generation. From the simulation results, it is seen that the missing power due to the variations in wind speed and solar radiation is supplied from the electrical grid to the loads. It is observed that the proposed system that comprises a micro-cogeneration system is able to work stably despite all the fluctuations in the output powers of other sources such as WECS and PV plant and load demand.

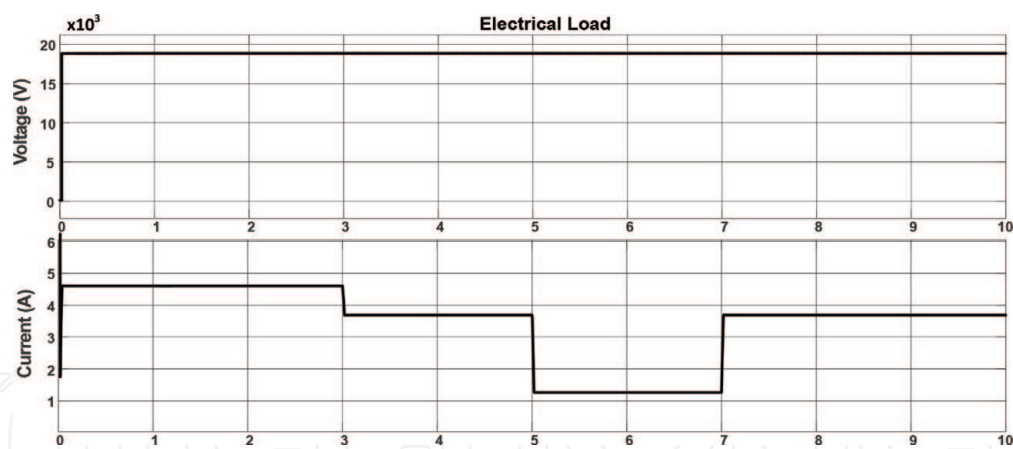


Figure 39.  
RMS voltage and RMS current of electrical load for case 7.

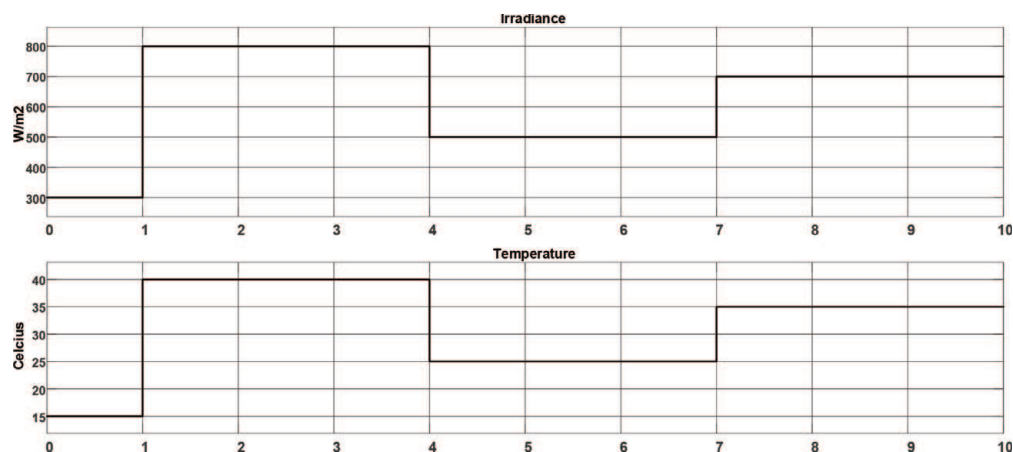


Figure 40.  
Graph of solar radiation and temperature for case 7.

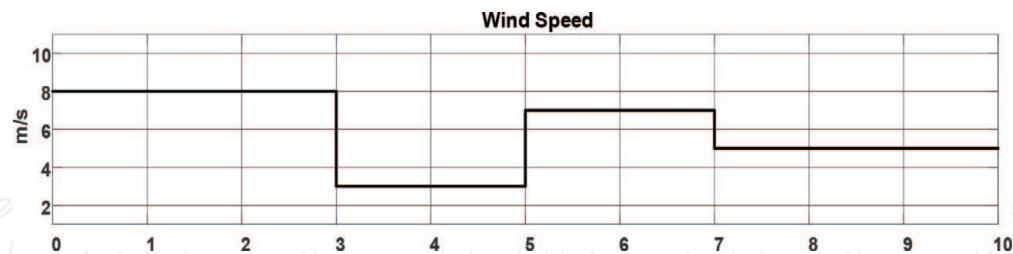


Figure 41.  
Graph of wind speed for case 7.

Cases	PV system	WECS	Load	Micro-cogeneration system	Grid
Case 1	10 kW	10 kW	−50 kW	30 kW	—
Case 2	[1,10] kW	10 kW	−50 kW	30 kW	[−9,0] kW
Case 3	[1,10] kW	[0,10] kW	−50 kW	30 kW	[−19,0] kW
Case 4	[1,10] kW	10 kW	[−50,−5] kW	30 kW	[−40,0] kW
Case 5	10 kW	[0,10] kW	[−70,−45] kW	30 kW	[0,35] kW
Case 6	10 kW	10 kW	[−70,−20] kW	30 kW	[−30,20] kW
Case 7	[1,10] kW	[0,10] kW	[−70,−20] kW	30 kW	[−20,35] kW

Table 3.  
Power generation and consumption values of the elements of the proposed system.

## 4. Conclusion

Renewable sources such as wind and solar have variable and intermittent characteristic by nature. For this reason, in microgrids supplied by these sources, there is a need for a compensating factor in order to ensure the stable operation of the microgrid for off-grid microgrids or the minimum energy demand from the electrical grid for on-grid microgrids. The expanding apprehension about climate change and energy subsection is driving specific policies to promote more efficient energy sources such as micro-cogeneration in many regions, particularly in the production of electricity. This paper proposes the use of micro-cogeneration system in a microgrid to support renewables in the microgrid.

The main contribution of this paper is that not only renewable energy sources such as solar and wind but also the micro-cogeneration system are used to supply electric energy. This study is carried out to analyze the operation of the micro gas turbine with solar and wind power generation systems. Firstly, a mathematical model of the micro gas turbine system, PV system, and WECS are given. After that, the control of the mentioned systems is explained. Lastly, the performance analysis of the proposed system is given via simulation results in seven different cases. The results show that the system is able to preserve the stable operation, while the parameters such as wind speed, solar radiation, temperature, and electrical load demand are changing.

## Author details

Kemal Aygul<sup>1</sup>, Burak Esenboga<sup>2</sup>, Abdurrahman Yavuzdeger<sup>3</sup>, Fırat Ekinci<sup>3</sup>,  
Tugce Demirdelen<sup>2\*</sup> and Mehmet Tumay<sup>2</sup>


<sup>1</sup> Department of Electrical and Electronics Engineering, Cukurova University, Adana, Turkey

<sup>2</sup> Department of Electrical and Electronics Engineering, Adana Alparslan Turkes Science and Technology University, Adana, Turkey

<sup>3</sup> Department of Energy Systems Engineering, Adana Alparslan Turkes Science and Technology University, Adana, Turkey

\*Address all correspondence to: [tdemirdelen@atu.edu.tr](mailto:tdemirdelen@atu.edu.tr)

## IntechOpen

© 2019 The Author(s). Licensee IntechOpen. Distributed under the terms of the Creative Commons Attribution - NonCommercial 4.0 License (<https://creativecommons.org/licenses/by-nc/4.0/>), which permits use, distribution and reproduction for non-commercial purposes, provided the original is properly cited. 

## References

- [1] Atmaca M. Efficiency analysis of combined cogeneration systems with steam and gas turbines. *Energy Sources, Part A: Recovery, Utilization, and Environmental Effects*. 2010;**33**(4): 360-369
- [2] Sağlam G, Tutum CC, Kurtulan S. A new PI tuning method for an industrial process: A case study from a micro-cogeneration system. *Energy Conversion and Management*. 2013;**67**:226-239
- [3] Lontsi F, Hamandjoda O, Fozao K, Stouffs P, Nganhon J. Dynamic simulation of a small modified Joule cycle reciprocating Ericsson engine for micro-cogeneration systems. *Energy*. 2013;**63**:309-316
- [4] Capaldi P, Daliento A, Rizzo R. Prototype of a 20 kW cogenerator with reduced global cost. In: 2014 49th International Universities Power Engineering Conference (UPEC). IEEE. 2014. pp. 1-6
- [5] Angrisani G, Marrasso E, Roselli C, Sasso M. A review on microcogeneration national testing procedures. *Energy Procedia*. 2014;**45**: 1372-1381
- [6] Dang TT, Ruellan M, Prévond L, Ahmed HB, Multon B. Sizing optimization of tubular linear induction generator and its possible application in high acceleration free-piston stirling microcogeneration. *IEEE Transactions on Industry Applications*. 2015;**51**(5): 3716-3733
- [7] Goyal R, Sharma D, Soni SL, Gupta PK, Johar D. An experimental investigation of CI engine operated micro-cogeneration system for power and space cooling. *Energy Conversion and Management*. 2015;**89**:63-70
- [8] Angrisani G, Canelli M, Roselli C, Sasso M. Microcogeneration in buildings with low energy demand in load sharing application. *Energy Conversion and Management*. 2015;**100**:78-89
- [9] Valenti G, Silva P, Fergnani N, Campanari S, Ravidà A, Di Marcoberardino G, et al. Experimental and numerical study of a micro-cogeneration Stirling unit under diverse conditions of the working fluid. *Applied Energy*. 2015;**160**:920-929
- [10] Mustafa KF, Abdullah S, Abdullah MZ, Sopian K, Ismail AK. Experimental investigation of the performance of a liquid fuel-fired porous burner operating on kerosene-vegetable cooking oil (VCO) blends for micro-cogeneration of thermoelectric power. *Renewable Energy*. 2015;**74**:505-516
- [11] Obi JB. State of art on ORC applications for waste heat recovery and micro-cogeneration for installations up to 100 kW<sub>e</sub>. *Energy Procedia*. 2015;**82**: 994-1001
- [12] Angrisani G, Canelli M, Roselli C, Sasso M. Integration between electric vehicle charging and micro-cogeneration system. *Energy Conversion and Management*. 2015;**98**:115-126
- [13] Darcovich K, Kenney B, MacNeil DD, Armstrong MM. Control strategies and cycling demands for Li-ion storage batteries in residential micro-cogeneration systems. *Applied Energy*. 2015;**141**:32-41
- [14] Najafi B, Mamaghani AH, Baricci A, Rinaldi F, Casalegno A. Mathematical modelling and parametric study on a 30 kW<sub>el</sub> high temperature PEM fuel cell based residential micro cogeneration plant. *International Journal of Hydrogen Energy*. 2015;**40**(3):1569-1583
- [15] Özgirgin E, Devrim Y, Albostan A. Modeling and simulation of a hybrid photovoltaic (PV) module-electrolyzer-PEM



fuel cell system for micro-cogeneration applications. *International Journal of Hydrogen Energy*. 2015;**40**(44): 15336-15342

[16] Najafi B, Mamaghani AH, Rinaldi F, Casalegno A. Fuel partialization and power/heat shifting strategies applied to a 30 kWel high temperature PEM fuel cell based residential micro cogeneration plant. *International Journal of Hydrogen Energy*. 2015; **40**(41):14224-14234

[17] Bouvier J-L, Michaux G, Salagnac P, Nepveu F, Rochier D, Kientz T. Experimental characterisation of a solar parabolic trough collector used in a micro-CHP (micro-cogeneration) system with direct steam generation. *Energy*. 2015;**83**:474-485

[18] Prinsloo G, Dobson R, Mammoli A. Model based design of a novel Stirling solar micro-cogeneration system with performance and fuel transition analysis for rural African village locations. *Solar Energy*. 2016;**133**:315-330

[19] Di Marcoberardino G, Roses L, Manzolini G. Technical assessment of a micro-cogeneration system based on polymer electrolyte membrane fuel cell and fluidized bed autothermal reformer. *Applied Energy*. 2016;**162**:231-244

[20] Zheng CY, Wu JY, Zhai XQ, Yang G, Wang RZ. Experimental and modeling investigation of an ICE (internal combustion engine) based micro-cogeneration device considering overheat protection controls. *Energy*. 2016;**101**:447-461

[21] Ferreira AC, Nunes ML, Teixeira JCF, Martins LASB, Teixeira SFCF. Thermodynamic and economic optimization of a solar-powered Stirling engine for micro-cogeneration purposes. *Energy*. 2016;**111**:1-17

[22] Bilgen S, Sarıkaya İ. The use and its impact on the environment of

cogeneration as an important element for a clean and sustainable energy future. *Energy Sources, Part A: Recovery, Utilization, and Environmental Effects*. 2017;**39**(21): 2078-2086

[23] Yu T, Tong J-P. Auto disturbance rejection control of microturbine system. In: *Power and Energy Society General Meeting-Conversion and Delivery of Electrical Energy in the 21st Century*, 2008 IEEE. 2008. pp. 1-6

[24] Li JJ. Modeling and simulation of micro gas turbine generation system for grid connected operation. In: *Power and Energy Engineering Conference (APPEEC), 2010 Asia-Pacific*. IEEE. 2010. pp. 1-4

[25] Gaonkar DN, Patel RN. Modeling and simulation of microturbine based distributed generation system. In: *2006 IEEE Power India Conference*. 2006. p. 5

[26] Bellia H, Youcef R, Fatima M. A detailed modeling of photovoltaic module using MATLAB. *NRIAG Journal of Astronomy and Geophysics*. 2014; **3**(1):53-61

[27] Singh G, Siwasia M, Vyas S, Kumar R. Implementation of a fuzzy logic based perturb and observe approach for maximum power point tracking of solar PV modules. In: *2016 IEEE 7th Power India International Conference (PIICON)*; IEEE. 2016. pp. 1-6

[28] Nedumgatt JJ, Jayakrishnan KB, Umashankar S, Vijayakumar D, Kothari DP. Perturb and observe MPPT algorithm for solar PV systems-modeling and simulation. In: *2011 Annual IEEE India Conference (INDICON)*; IEEE. 2011. pp. 1-6

[29] Hur S. Modelling and control of a wind turbine and farm. *Energy*. 2018; **156**:360-370

[30] Mosa MA, Elsyed AA, Amin AM, Ghany AA. Variable speed wind turbine pitch angle controller with rate limiter anti-windup. In: 2016 Eighteenth International Middle East Power Systems Conference (MEPCON); IEEE. 2016. pp. 95-100

[31] Dhar MK, Thasfiquzzaman M, Dhar RK, Ahmed MT, Al Mohsin A. Study on pitch angle control of a variable speed wind turbine using different control strategies. In: 2017 International Conference on Power, Control, Signals and Instrumentation Engineering (ICPCSI); IEEE. 2017. pp. 285-290